PCCP

ROYAL SOCIETY OF CHEMISTRY

PAPER

View Article Online
View Journal

Cite this: DOI: 10.1039/d2cp05498a

Stability of sulfur molecules and insights into sulfur allotropy†

Maria Fedyaeva, *[ab] Sergey Lepeshkin[bcd] and Artem R. Oganov [c]

Received 24th November 2022,
Accepted 6th March 2023

DOI: 10.1039/d2cp05498a

rsc.li/pccp

Using *ab initio* evolutionary algorithm USPEX, we predict structures of sulfur molecules S_n (n = 2 – 21). It is shown that for $n \geq 5$ stable structures of sulfur molecules are closed helical rings, which is in agreement with the experimental data and previous calculations. We investigate the stability of molecules using the following criteria: second-order energy difference (Δ^2E), fragmentation energy (E_{frag}) and HOMO–LUMO gaps. The S_8 molecule has the highest value of Δ^2E and forms the most common allotropic form of sulfur (orthorhombic α-S), into which all other modifications convert over time at room temperature. Commonly found molecules S_{12} and S_6 also have strongly positive Δ^2E. Another well-known molecule, S_7, has negative Δ^2E, but at temperatures above 900 K has positive second-order free energy difference Δ^2G. Generally, Δ^2E (or Δ^2G at finite temperatures) is a quantitative measure of the stability allowing one to predict the ease of formation of molecules and corresponding molecular crystals. Temperature dependence of the above-mentioned measures of stability explains a wide range of facts about sulfur crystalline allotropes, molecules in the gas phase, *etc.*

Introduction

Elemental sulfur occurs in more allotropic forms than any other element in the periodic table except, perhaps, carbon.[1] In nature, α- and β-allotropes are formed, and both are made of S_8 molecules. However, other allotropes, based on other S_n molecules and less stable at normal conditions, have also been obtained in the experiment.

Sulfur molecules with different numbers of sulfur atoms are also known experimentally and have been found in complex minerals. For example, the S_3, S_4, and S_5 molecules have been found in sodalite group minerals.[2] Sulfur clusters can give color to minerals: the bright blue color of lazurite is due to the chromophore ion $S_3^{\bullet -}$.[3] The green color of slyudyankaite ($Na_{28}Ca_4(Si_{24}Al_{24}O_{96})(SO_4)_6(S_6)_{1/3}(CO_2)\cdot 2H_2O$) has been explained by the presence of two sulfur clusters—S_6 (yellow chromophore) and $S_3^{\bullet -}$ (blue chromophore). Also, according to the spectroscopic data, slyudyankaite contains impurities of the chromophore clusters S_4—centers of red and lilac color.[2]

Applications of sulfur molecules in technology are currently on the rise. For example, to improve the electrochemical performance of modern lithium–sulfur batteries, graphene nanocages are filled with S_8 in the inner cavity and S_2–S_4 molecules in the shell of the cage.[4] Sulfur molecules S_4 and S_5, attached to activated carbon, improve the mercury adsorption from flue gas,[4,5] which can help to control Hg emissions. Also sulfur can help in the extraction of gold from cyanides.[6]

In this paper we find ground-state structures of small- to medium-sized sulfur molecules (from S_2 to S_{21}) and quantitatively estimate their stability using criteria borrowed from studies of nanoparticles (such as second-order energy differences and fragmentation energies). For molecules containing different numbers of atoms, we compare the obtained values with the likelihood of the formation of the molecule, as well as the thermodynamic stability and ease of synthesis of the corresponding molecular crystals.

Computational methodology

To find the most stable structures of sulfur molecules, we used the evolutionary algorithm USPEX[7–9] (see also **https://uspex-team.org**) coupled with *ab initio* calculations. This method allows one to predict the structure of both stable and metastable molecules and crystals without requiring any experimental data. During the calculation, a set of structures (called "population") evolves in order to maximize stability. An initial generation is produced using a random symmetric structure

[a] *Moscow State University, Leninskie Gory, Moscow 119991, Russia. E-mail: femaal.femaal3@yandex.ru*
[b] *Vernadsky Institute of Geochemistry and Analytical Chemistry, Russian Academy of Sciences, Kosygina, 19, Moscow, 119991, Russia*
[c] *Skolkovo Institute of Science and Technology, Bolshoy Boulevard 30, bld. 1, Moscow, 121205, Russia*
[d] *Lebedev Physical Institute, Russian Academy of Sciences, 53 Leninskii prosp., 119991, Moscow, Russia*

† Electronic supplementary information (ESI) available. See DOI: **https://doi.org/10.1039/d2cp05498a**

generator, and structures are relaxed and ranked by energy. The most energetically unfavorable ones are rejected, whereas the remaining ones are used as parents to produce the next generation of structures using such variation operators as heredity (matching random slices of the parent structures), softmutation, and add/remove mutations, as well as random symmetric structure generator. Here we use the recently developed technique[10] for simultaneous global optimization of molecules within a wide range of compositions. The approach efficiently exploits the exchange of structural motifs between molecules of different compositions and works several times faster than traditional techniques where each composition is processed separately.

Structure relaxations were performed using the spin-polarized PBE functional[11] as implemented in the VASP code.[12] In these calculations, we used the projector augmented wave method[13] and 260 eV plane wave energy cutoff. To model molecules using a periodic code, the supercell method was employed, where periodic images of a molecule were separated by a vacuum layer with a thickness of 10 Å to ensure that the interaction between periodic images of the molecules is negligible. For 10 lowest-energy isomers of each composition, structures were again relaxed and energies recomputed using a more accurate (but more expensive) approach. This final refinement was done using the Becke three-parameter hybrid functional with the Lee–Yang–Parr nonlocal correlation functional (B3LYP)[14] and 6-311+G(d,p) basis set[15] with the Gaussian 16 code.[16] In these calculations, the electronic structure problem was solved for isolated molecules. All values discussed in this paper, unless noted otherwise, were obtained in these B3LYP calculations.

Results and discussion

The ground-state structures of all calculated S_n molecules, with the number of atoms n from 2 to 21, are presented in Fig. 1. Their atomic coordinates and total energies are given in ESI† (Section S1). We also calculated the vibrational spectra for each molecule (see ESI,† Section S2) and verified that there are no imaginary frequencies. The structures are either the same or more energetically favorable than ones from previous studies.[1,17,18] For example, for the S_4 molecule, the structure of which is still debated (chain or ring configuration), we have shown that the chain form is more favorable. Another interesting case is the S_6 molecule, for which we found that armchair conformation is more energetically favorable than boat conformation by 0.53 eV. In addition, for S_{15}, S_{17}, S_{18}, S_{19} and S_{20} molecules we found structures which are by 0.17, 0.12, 0.32, 0.09 and 0.10 eV, respectively, energetically more favorable than previously predicted ones.[18] This attests to the high robustness of our structure prediction method.

We found that for molecules with the number of atoms $n \leq 4$, the stable form is an open chain, whereas for those with $n \geq 5$, rings are more favorable. Large S_n molecules are elongated rings, consisting of roughly parallel chains, the interaction between which stabilizes such shape. The tendency to form rings can be explained by the octet rule, which dictates that the coordination number of sulfur be $8–N = 2$, where N is the number of valence electrons, so each sulfur atom must have two neighbors. Therefore, pure sulfur avoids structures with terminal atoms and forms cyclic molecules (or infinite chains) in which each atom has two neighbors.

We have calculated the following energetic characteristics of S_n molecules: atomization energy (E_{at}), second-order differences of energy ($\Delta^2 E$) and fragmentation energies (E_{frag}), which are traditionally used in studies of nanoclusters[19,20] and allow one to estimate the stability of compounds. Taking into account the vibrational, translational and rotational entropic effects, finite-temperature generalizations of these values were calculated at different temperatures (T = 0, 300, 600, 1000, 1500 K); at finite temperatures one should use the Gibbs free energy (G) instead of the energy (E). Further in the text, we discuss these characteristics at zero temperature, and then characterize the patterns of their change with increasing temperature. Fig. 2a shows the atomization energies of sulfur molecules:

$$E_{at} = (E_n - nE_1)/n \quad (1)$$

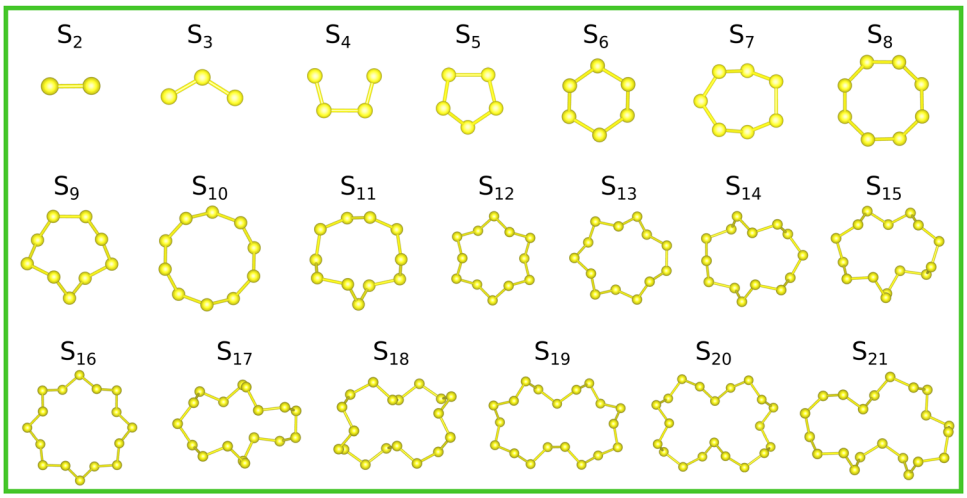

Fig. 1 Lowest-energy structures of sulfur molecules S_n (n = 2–21).

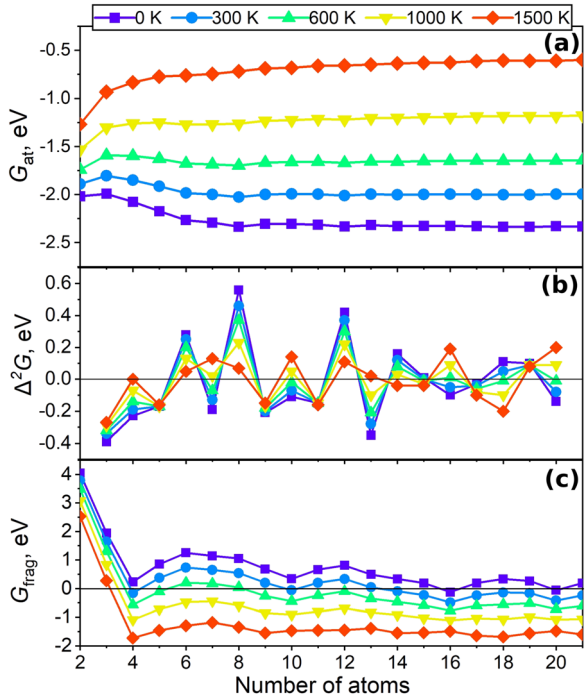

Fig. 2 Thermodynamics of sulfur molecules (a) Atomization energies; (b) second-order differences of energy and (c) fragmentation energies of S_n molecules (n = 2–21). These energetic characteristics are shown at different temperatures (T = 0, 300, 600, 1000, 1500 K), at finite temperatures one should use the Gibbs free energy (G) instead of the energy (E).

where n – number of atoms in the molecule, E_n – the energy of the molecule, and E_1 – the energy of an isolated atom in its ground state. Note that eqn (1) differs from the conventional definition of the atomization energy by sign; this is more convenient for our purposes. A careful look at it reveals that the energy alone is not a good criterion for predicting the favorability of a given composition. For example, S_7 has lower energy than the much more common S_6 (Fig. 2a).

Also, while the energies of the S_7 and S_8 molecules differ by only about 0.1 eV/atom, the difference in the ease of obtaining them is enormous. Even more strikingly, extremely rare large molecules S_{18} and S_{19} have lower energy (by 2–3 meV/atom) than the S_8 molecule. However, S_8 is an incomparably more common form. Since direct comparison of atomization energies is meaningless, and one should use some measures of conditional stability.

The relative stability of molecules can be explored using the second-order difference of energy, Δ^2E:

$$\Delta^2E = E_{n+1} + E_{n-1} - 2E_n \quad (2)$$

where E_n is the total energy of the molecule containing n atoms. This quantity characterizes local stability and measures the resistance towards the transfer of one atom between two identical molecules during their collision. Molecules having a positive Δ^2E are called "magic". The values of the second-order difference of energy Δ^2E for the S_n molecules (n = 2–21) are shown in Fig. 2b.

Numerous studies of nanoclusters have shown that clusters with high values of Δ^2E produce peaks in mass spectra.[21–24] Sulfur is particularly interesting because it forms molecular crystals, which can be thought to be made of the molecules that are most abundant prior to crystallization. Below we analyze the relationship between magicity (*i.e.* stability relative to nearest compositions, eqn (1)) of molecules and their abundance in various sulfur allotropes and other experimentally studied systems, moving in the order of decreasing stability (understood in terms of the ease of synthesizing and retaining these molecules, and quantified in terms of Δ^2E).

The most common and most stable natural allotrope of sulfur is the yellow orthorhombic α-form, to which all other modifications eventually revert at room temperature. It is made of S_8 molecules, which have the "Saxon crown" structure, and this matches our prediction perfectly. The calculations show that the most stable molecule is S_8 and its second-order difference of energy is 0.66 eV. The calculated S–S bond length and angle are 2.06 Å and 109.5°, whereas those determined experimentally are 2.04 Å and 107.8°, respectively. Each sulfur atom has a tetrahedral configuration: based on the octet rule, it has two bonds to neighboring atoms and two lone electron pairs. According to the VSEPR (valence shell electron pair repulsion model),[25] the bond angle should be close to 109.47°. The proximity of the bond angles to the ideal is one of the reasons for particular stability of the S_8 molecules. In other molecules, we find different bond angles: 103° in S_6, 112° in S_{10}, 108.5° in S_{12}, and so forth.

S_{12} molecules have the second largest Δ^2E are the second by stability both in our calculations and second most common in experiment. In synthesis of other sulfur molecules, S_{12} is often an accompanying product, together with S_8, S_{10}, and S_6 molecules, which indicates their particular stability as well. Crystallized S_{12} is a pale-yellow solid which melts at 145–147 °C.[26]

S_6, S_{10}, and S_{14} molecules are also stable, but their Δ^2E are lower than those of S_8 or S_{12}. One of the first sulfur rings characterized experimentally both in solid state and in isolated sulfur molecules, S_6 forms orange rhombohedral crystals stable up to 50 °C, above which it transforms into S_8.[27] S_6 molecules are found in cages within the structures of sodalite group minerals, for example, in slyudyankaite.[2] These molecules are yellow chromophores (responsible for the rich yellow color). It has been predicted that the S_6 crystal is a stable high-pressure phase in the pressure range of 7–18 GPa at 0 K.[7] S_{10} molecules occur as a minor component of liquid sulfur. Monoclinic crystals of *cyclo*-decasulfur have been obtained in experiment. Pure S_{10} has an olive green color.[28] Also, very interesting co-crystals $S_{10}{\cdot}S_6$ are known, in which layers of S_6 and S_{10} molecules alternate. The mean interatomic distance and bond angles in the S_{10} molecules are close to those in *cyclo*-S_{12}. S_{14} molecules can be obtained in experiment and are known as intense-yellow rodlike crystals. S_{14} can be kept stable at ambient conditions in its crystalline form for days, after which it decomposes into S_8 and S_7.[28]

The smallest molecules S_2–S_5 have been detected in sulfur vapor at high temperatures. They have been studied using

Raman spectroscopy after matrix isolation in an inert gas. The sulfur dimer has the same structure as O_2 and S_3 structure is similar to the structure of ozone because of their similar electronic configuration. Tetrasulfur has been also detected in liquid sulfur and in the atmosphere of Jupiter's moon Io, but it does not occur naturally on Earth. S_5 is very unstable due to the high bond strains in the ring structure, but it was found in samples of liquid sulfur.[28] No definitive experimental structural information is available for the S_4 and S_5 molecules.

Four crystalline (α-S_7, β-S_7, γ-S_7, and δ-S_7) modifications based on S_7 molecules are metastable up to 39 °C. Since S_7 rapidly decomposes into S_6 and S_8[27] above 20 °C, it needs to be handled with cooling and should be stored at temperatures below −50 °C[17] (S_7 molecules can exist at room temperature as separate molecules if stabilized by certain solvents). Crystals of native elemental sulfur also quite often contain traces of S_7 (up to 0.3%).[29] S_9 molecules form two crystalline polymorphs, always found in coexistence with each other. They occur naturally in liquid sulfur samples and as a minor contaminant in samples of α-sulfur.[28] The less common molecules S_{11} and S_{13} occur only as minor components of liquid sulfur and irradiated sulfur solutions (irradiation by a high-pressure mercury lamp (200–600 nm)).[30] S_{11} can also be synthesized in the laboratory.[28] S_{15} molecules form a crystalline phase, obtained as a lemon-yellow powder, and its crystal structure has not been determined yet.

The S_n allotropes (n = 16, 17, 19, $n > 20$) have not yet been obtained in pure forms; however, a mixture of large sulfur rings S_n, where n = 12–35, has been observed. From the mixture of S_n rings, pure S_{18} and S_{20} have been obtained, and their infrared and Raman spectra have been measured.[17,31]

From the above analysis it is clear that in general using the value of $\Delta^2E(n)$ one can estimate the likelihood of the formation of the S_n molecule and of the corresponding molecular crystals. All the well-known stable sulfur allotropes consist of magic molecules.

Another criterion to evaluate the stability is the fragmentation energy (E_{frag}). It is defined as follows: from all possible fragmentation channels into two fragments $S_n \rightarrow S_k + S_{n-k}$ ($1 \leq k \leq n-1$) we choose the most energetically favorable one:

$$E_{frag}(n) = \min_k\{E_{frag}(n, k)\}, \quad (3)$$

where $E_{frag}(n, k) = E(k) + E(n-k) - E(n)$. The higher E_{frag}, the more resistant the S_n molecule is to fragmentation. The graph $E_{frag}(n)$ is shown in Fig. 2c; a complete set of fragmentation energies and fission products is given in ESI† Table S1. For S_n molecules with n = 3–11 the most favorable products of fragmentation include the S_2 molecule, for n = 12–14 – the S_6 molecule, and for n = 14–21 (and probably for all larger ones) – S_8 molecule, which indicates the special stability of these molecules and ease of their formation.

Next, we analyze the change in the considered characteristics (G_{at}, Δ^2G and G_{frag}) with increasing temperature. First of all, it is worth noting that at normal conditions ($T \sim 300$ K) the values of energetic characteristics are close to these at 0 K, but at high temperatures the differences are large.

Concerning the free energy of atomization (G_{at}), at zero Kelvin one can see its overall decrease (to more negative, *i.e.* more favorable, values) with increasing number of atoms (see Fig. 2a), with S_8, S_{12} and larger ones having the most negative values. As temperature rises, the pattern changes to the opposite, and small molecules become more stable than larger ones. For example, at temperatures above ∼1000 K, S_2 becomes the most stable molecule, which is in agreement with experimental and theoretical data.[32,33]

As for the Δ^2G graph, with increasing temperature it smoothes out, *i.e.* its absolute values decrease. Moreover, for some molecules the value of Δ^2G change the sign. This is the case of, for example, the S_7 molecule: its Δ^2G is negative at low temperatures, but becomes positive at temperatures above ∼900 K. This is in agreement with experimental data, according to which S_7 has increased abundance at such temperatures.

$G_{frag}(n)$ is positive at zero Kelvin for all n, except n = 16 and 20 (these molecules decompose into very stable fragments: $S_{16} \rightarrow S_8 + S_8$ and $S_{20} \rightarrow S_{12} + S_8$). As temperature rises, molecules become less and less stable against fragmentation, and at temperatures above ∼1000 K, G_{frag} is negative for all molecules except S_2 and S_3. This is consistent with the higher abundance of S_2 and S_3 molecules in sulfur vapor at high temperatures.

We have also calculated the energy gaps between highest occupied and lowest unoccupied molecular orbitals (HOMO–LUMO gaps) of the S_n molecules (see Fig. 3). As electronic polarization is related to excitation of electrons into unoccupied levels, the HOMO–LUMO gap characterizes the polarizability of molecules. Also, wide HOMO–LUMO gaps indicate closed-shell electronic structure and relatively high chemical inertness, both of which are indicative of stability. Indeed, S_8 molecule has the largest HOMO–LUMO gap, 4.58 eV. The S_{12}, S_6, and S_{10} molecules are next in terms of the HOMO–LUMO gap, which agrees with their high second-order energy differences (Δ^2E) and experimental data. In addition, one can notice the similarity between graphs of E_{frag} and HOMO–LUMO gap. One should note that the HOMO–LUMO gap of 4.58 eV for the isolated S_8 molecule should make it colorless: with such gap it cannot absorb photons in the energy range of visible light

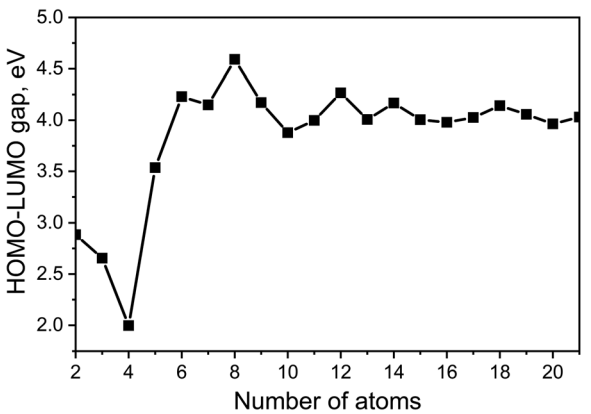

Fig. 3 HOMO–LUMO gaps for S_n molecules (n = 2–21)

(1.8–3.1 eV). At the same time, crystalline α-S (made of S_8 molecules) has light yellow color. In a crystal, molecular orbitals overlap and broaden into bands, and one can expect the band gap in α-S to be smaller than HOMO–LUMO gap in the S_8 molecule. To calculate the band gap of crystalline sulfur we chose the modified Becke-Johnson meta-GGA functional, known to give the most accurate band gaps of solids.[34,35] For the band gap of α-S the result is 2.73 eV, consistent with yellow color and with an earlier experimental result of 2.79 eV[33] and with yellow color of crystalline sulfur.

Conclusions

We have predicted the optimal atomic structures of sulfur molecules containing 2–21 atoms using the evolutionary algorithm USPEX and *ab initio* calculations. For each molecule we calculated the second-order energy difference Δ^2E as a measure of its stability, as well as atomization and fragmentation energies (E_{at} and E_{frag}) and HOMO–LUMO gap.

In previous studies, it has been shown that clusters with positive Δ^2E correspond to particularly high peaks in mass spectra and can be called ''magic''. In this paper we have shown that magic molecules play a special role in the structural chemistry and geochemistry of sulfur. The most stable sulfur crystals consist of magic molecules, and by the value of Δ^2E we can estimate the likelihood of making such molecules. All low-pressure crystalline sulfur allotropes have molecular crystal structures. As it is easier to grow the crystal from the most abundant molecules, nearly all known sulfur allotropes are made of magic molecules (such as S_8, S_{12}, S_6 and others). This rule can also be applied to other molecular crystals, because individual molecules in them are weakly bound to each other.

Taking into account vibrational and entropic effects, we have calculated the proposed stability measures at different temperatures. The obtained values (G_{at}, Δ^2G and G_{frag}) can be used for predicting which molecules will be the most abundant at different temperatures. For example, thermal effects make the S_7 molecule magic, thus explaining its appearance in experiments.

This approach also allows one to predict stable molecules or ions encaged in other crystals. For example, the most favorable in terms of Δ^2E among charged sulfur molecules (S_n^-) is the S_3^- ion.[18] As shown in study[3], S_3^- ions (blue chromophores) are common inside large cages of sodalite-group minerals (e.g. lazurite and slyudyankaite) and play a major role in determining the color of these minerals.

Conflicts of interest

There are no conflicts to declare.

Acknowledgements

Global structure optimization was supported by the Russian Science Foundation (Grant 19-72-30043). The calculations were performed on Oleg and Arkuda supercomputers at Skoltech and at the Joint Supercomputer Center of the Russian Academy of Sciences. The stability analysis was performed within the Project of the State Assignment (Vernadsky Institute of Geochemistry and Analytical Chemistry of Russian Academy of Sciences, Moscow, Russia). We thank Prof. N.V. Chukanov for illuminating discussions.

References

1 N. N. Greenwood and A. Earnshaw, *Chemistry of the Elements*, Elsevier, 2012.
2 N. V. Chukanov, N. V. Zubkova, I. V. Pekov, R. Y. Shendrik, D. A. Varlamov, M. F. Vigasina, D. I. Belakovskiy, S. N. Britvin, V. O. Yapaskurt and D. Y. Pushcharovsky, Sapozhnikovite, $Na_8(Al_6Si_6O_{24})(HS)_2$, a new sodalite-group mineral from the Lovozero alkaline massif, Kola Peninsula, *Mineral. Mag.*, 2022, **86**, 49–59.
3 N. V. Chukanov, M. F. Vigasina, N. V. Zubkova, I. V. Pekov, C. Schäfer, A. V. Kasatkin, V. O. Yapaskurt and D. Y. Pushcharovsky, Extra-Framework Content in Sodalite-Group Minerals: Complexity and New Aspects of Its Study Using Infrared and Raman Spectroscopy, *Minerals*, 2020, **10**, 363.
4 Y. Yuan, G. Tan, J. Wen, J. Lu, L. Ma, C. Liu, X. Zuo, R. Shahbazian-Yassar, T. Wu and K. Amine, Encapsulating Various Sulfur Allotropes within Graphene Nanocages for Long-Lasting Lithium Storage, *Adv. Funct. Mater.*, 2018, **28**, 1706443.
5 R. Sun, G. Luo, X. Li, H. Tian and H. Yao, Theoretical research on role of sulfur allotropes on activated carbon surface in adsorbing elemental mercury, *Chem. Eng. J.*, 2021, **404**, 126639.
6 Y. Zia, S. Mohammadnejad and M. Abdollahy, Gold passivation by sulfur species: A molecular picture, *Miner. Eng.*, 2019, **134**, 215–221.
7 A. R. Oganov and C. W. Glass, Crystal structure prediction using ab initio evolutionary techniques: principles and applications, *J. Chem. Phys.*, 2006, **124**, 244704.
8 A. R. Oganov, A. O. Lyakhov and M. Valle, How evolutionary crystal structure prediction works--and why, *Acc. Chem. Res.*, 2011, **44**, 227–237.
9 A. O. Lyakhov, A. R. Oganov, H. T. Stokes and Q. Zhu, New developments in evolutionary structure prediction algorithm USPEX, *Comput. Phys. Commun.*, 2013, **184**, 1172–1182.
10 S. V. Lepeshkin, V. S. Baturin, Y. A. Uspenskii and A. R. Oganov, Method for Simultaneous Prediction of Atomic Structure and Stability of Nanoclusters in a Wide Area of Compositions, *J. Phys. Chem. Lett.*, 2019, **10**, 102–106.
11 J. P. Perdew, K. Burke and M. Ernzerhof, Generalized Gradient Approximation Made Simple, *Phys. Rev. Lett.*, 1996, **77**, 3865–3868.
12 G. Kresse and J. Furthmüller, Efficient iterative schemes for ab initio total-energy calculations using a plane-wave basis set, *Phys. Rev. B: Condens. Matter Mater. Phys.*, 1996, **54**, 11169–11186.

13 P. E. Blöchl, Projector augmented-wave method, *Phys. Rev. B: Condens. Matter Mater. Phys.*, 1994, **50**, 17953–17979.
14 M. E. Casida, C. Jamorski, K. C. Casida and D. R. Salahub, Molecular excitation energies to high-lying bound states from time-dependent density-functional response theory: Characterization and correction of the time-dependent local density approximation ionization threshold, *J. Chem. Phys.*, 1998, **108**, 4439–4449.
15 P. J. Stephens, F. J. Devlin, C. F. Chabalowski and M. J. Frisch, Ab initio calculation of vibrational absorption and circular dichroism spectra using density functional force fields, *J. Phys. Chem.*, 1994, **98**, 11623–11627.
16 M. J. Frisch, G. W. Trucks, H. B. Schlegel, G. E. Scuseria, M. A. Robb, J. R. Cheeseman, G. Scalmani, V. Barone, G. A. Peters-son, H. Nakatsuji, X. Li, M. Caricato, A. V. Marenich, J. Bloino, B. G. Janesko, R. Gomperts, B. Mennucci, H. P. Hratchian, J. V. Ortiz, A. F. Izmaylov, J. L. Sonnenberg, D. Williams-Young, F. Ding, F. Lipparini, F. Egidi, J. Goings, B. Peng, A. Petrone, T. Henderson, D. Ranasinghe, V. G. Zakrzewski, J. Gao, N. Rega, G. Zheng, W. Liang, M. Hada, M. Ehara, K. Toyota, R. Fukuda, J. Hasegawa, M. Ishida, T. Nakajima, Y. Honda, O. Kitao, H. Nakai, T. Vreven, K. Throssell, J. A. Montgomery, Jr., J. E. Peralta, F. Ogliaro, M. J. Bearpark, J. J.Heyd, E. N. Brothers, K. N. Kudin, V. N. Staroverov, T. A. Keith, R. Kobayashi, J. Normand, K. Raghavachari, A. P. Ren-dell, J. C. Burant, S. S. Iyengar, J. Tomasi, M. Cossi, J. M.Millam, M. Klene, C. Adamo, R. Cammi, J. W. Ochterski, R. L. Martin, K. Morokuma, O. Farkas, J. B. Foresman and D. J. Fox, *Gaussian 16 Revision C.01*, Gaussian Inc., Wallingford CT, 2016.
17 R. Steudel and B. Eckert, Elemental Sulfur and Sulfur-Rich Compounds I, *Top. Curr. Chem.*, 2003, **230**, 1–134.
18 Y. Jin, G. Maroulis, X. Kuang, L. Ding, C. Lu, J. Wang, J. Lv, C. Zhang and M. Ju, Geometries, stabilities and fragmental channels of neutral and charged sulfur clusters: $S_n(Q)$ (n = 3–20, Q = 0, ±1), *Phys. Chem. Chem. Phys.*, 2015, **17**, 13590–13597.
19 A. Arab and M. Habibzadeh, Theoretical study of geometry, stability and properties of Al and AlSi nanoclusters, *J. Nanostruct. Chem.*, 2016, **6**, 111–119.
20 Z. Hashemi, S. Rafiezadeh, R. Hafizi, S. J. Hashemifar and H. Akbarzadeh, First-principles study of MoS2 and MoSe2 nanoclusters in the framework of evolutionary algorithm and density functional theory, *Chem. Phys. Lett.*, 2018, **698**, 41–50.
21 X.-P. Li, W.-C. Lu, Q.-J. Zang, G.-J. Chen, C. Z. Wang and K. M. Ho, Structures and stabilities of Pb(n) (n <or= 20) clusters, *J. Phys. Chem. A*, 2009, **113**, 6217–6221.
22 C. P. Poole Jr and F. J. Owens, *Introduction to Nanotechnology*, John Wiley & Sons, 2003.
23 C. Rajesh, C. Majumder, M. G. R. Rajan and S. K. Kulshreshtha, Isomers of small Pbn clusters (n = 2–15): Geometric and electronic structures based on ab initio molecular dynamics simulations, *Phys. Rev. B: Condens. Matter Mater. Phys.*, 2005, **72**, 235411.
24 Y. Wang, Y. Zhou, Y. Zhang and W. E. Buhro, Magic-size II-VI nanoclusters as synthons for flat colloidal nanocrystals, *Inorg. Chem.*, 2015, **54**, 1165–1177.
25 R. J. Gillespie and I. Hargittai, *The VSEPR Model of Molecular Geometry*, Courier Corporation, 2013.
26 E. Zysman-Colman, P. Leste-Lassere and D. N. Harpp, Probing the chemistry of rare sulfur allotropes: S9, S12 and S20, *J. Sulfur Chem.*, 2008, **29**, 309–326.
27 E.-M. Strauss and R. Steudel, Photolyse von elementarem schwefel (S6, S7, S8, S10, S12) in kohlenstoffdisulfidlösung [1]/photolysis of elemental sulfur (S6, S7, S8, S10, S12) in carbondisulfide solution [1], *Z. Naturforsch., B: J. Chem. Sci.*, 1987, **42**, 682–690.
28 Website, **https://wiki.aalto.fi/display/SSC/Allotropy+of+sulfur**.
29 R. Steudel and B. Holz, Detection of reactive sulfur molecules (S6, S7, S9, S_∞) in commercial sulfur, in sulfur minerals, and in sulfur melts slowly cooled to 20 °C [1], *Z. Naturforsch. B: J. Chem. Sci.*, 1988, **43**, 581–589.
30 D. Hohl, R. O. Jones, R. Car and M. Parrinello, Structure of sulfur clusters using simulated annealing: S2 to S13, *J. Chem. Phys.*, 1988, **89**, 6823–6835.
31 B. Eckert and R. Steudel, Molecular Spectra of Sulfur Molecules and Solid Sulfur Allotropes, *Top. Curr. Chem.*, 2003, 31–98.
32 B. Meyer, Elemental Sulfur, *Chem. Rev.*, 1976, **76**(3), 367–388.
33 A. J. Jackson, D. Tiana and A. Walsh, A universal chemical potential for sulfur vapours, *Chem. Sci.*, 2016, **7**, 1082–1092.
34 T. Rauch, M. A. L. Marques and S. Botti, Local Modified Becke-Johnson Exchange–Correlation Potential for Interfaces, Surfaces, and Two-Dimensional Materials, *J. Chem. Theory Comput.*, 2020, **16**, 2654–2660.
35 W. Zulfiqar, S. M. Alay-e-Abbas, G. Abbas, A. Laref, J. A. Larsson and A. Shaukat, Revisiting the structural, electronic and photocatalytic properties of Ti and Zr based perovskites with meta-GGA functionals of DFT, *J. Mater. Chem. C*, 2021, **9**, 4862–4876.

